

**EFFECT OF COLD WALL ON LAMINAR FREE
CONVECTION ACROSS A HORIZONTAL
CYLINDER WITH PART ADIABATIC
SURFACE**

A Dissertation Submitted in Partial fulfillment of the
requirements for the award of the degree
of

Master of Philosophy



By

MD. ABDUL ALIM

Registration no. 9409005, Session 1993-95

Department of Mathematics

Bangladesh University of Engineering and Technology

Dhaka-1000



The thesis entitled

**EFFECT OF COLD WALL ON LAMINAR FREE CONVECTION ACROSS
A HORIZONTAL CYLINDER WITH PART ADIABATIC SURFACE**

Submitted


By

MD ABDUL ALIM

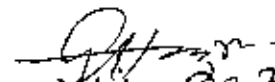
Registration no 9409005, Session 1993-94-95, a part time student of M. Phil
(Mathematics) has been accepted as satisfactory in partial fulfillment for the Degree
of Master of Philosophy in Mathematics on 27th September, 2000 by the


Board of Examiners

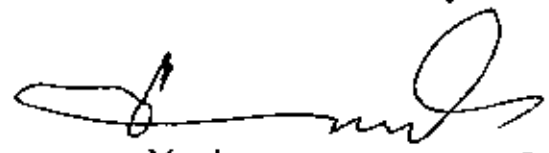
1. **Dr. Md. Mustafa Kamal Chowdhury**
Associate Professor
Department of Mathematics,
BUET, Dhaka-1000
2. **Dr. A. K. M. Sadrul Islam**
Professor
Department of Mechanical Engineering
BUET, Dhaka-1000
3. **A. K. Mazra**
Head,
Department of Mathematics
BUET, Dhaka-1000
4. **Md. Isa**
Associate Professor
Department of Mathematics
BUET, Dhaka-1000
5. **Dr. Gazi Md. Khalil**
Professor, Department of Naval
Architecture and Marine Engineering
BUET, Dhaka-1000


Supervisor


Co-Supervisor


Member 27.2.2001


Member 27/2


Member
(External) 27-2-2001

The thesis entitled
**EFFECT OF COLD WALL ON LAMINAR FREE CONVECTION ACROSS
A HORIZONTAL CYLINDER WITH PART ADIABATIC SURFACE**

Submitted

By

MD. ABDUL ALIM

Registration no. 9409005, Session 1993-94-95, a part time student of M. Phil (Mathematics) has been accepted as satisfactory in partial fulfillment for the Degree of Master of Philosophy in Mathematics on 27th September, 2000 by the

Board of Examiners

- | | |
|---------------------------------------------------------------------------------------------------------------------|----------------------|
| 1. Dr. Md. Mustafa-Kamal Chowdhury
Associate Professor
Department of Mathematics,
BUET, Dhaka-1000 | Supervisor |
| 2. Dr. A. K. M. Sadrul Islam
Professor
Department of Mechanical Engineering
BUET, Dhaka-1000 | Co-Supervisor |
| 3. A. K. Hazra
<i>Head,</i>
Department of Mathematics
BUET, Dhaka-1000 | Member |
| 4. Md. Isa
Associate Professor
Department of Mathematics
BUET, Dhaka-1000 | Member |
| 5. Dr. Gazi Md. Khalil
Professor, Department of Naval
Architecture and Marine Engineering
BUET, Dhaka-1000 | Member
(External) |

Contents

Acknowledgements	i
Abstract	ii
Nomenclature	iii-iv
List of figures	v-vi
Chapter 1	
1.1 Introduction	1-5
Chapter 2	
2.1 Mathematical Formulation	6
2.2 Transformation of the equations	7
Chapter 3	
3 Methods of Solutions	10
3.1 Perturbation solution method for smaller ξ	10
3.2 Integral solution method	14
3.3 Finite Volume method	17

Chapter 4

Results and discussion 35-37

Conclusions 37-38

Appendix-A 39-43

Appendix-B 44-48

References 49-50

Acknowledgement

I would like to express my profound gratitude and appreciation to the supervisor of this dissertation Dr. Md. Mustafa Kamal Chowdhury, Associate Professor, Department of Mathematics, BUET, and the co-supervisor Dr. A. K. M. Sadrul Islam, Professor, Department of Mechanical Engineering, Bangladesh University of Engineering and Technology (BUET), Dhaka-1000, Bangladesh whose generous help, guidance, constant encouragement and indefatigable assistance were available at all stages of my research work. I am so grateful to them for their earnest feeling and helps in matters concerning my research affairs.

I express my deep regards to my respectable teacher A. K. Hazra, Head of the Department of Mathematics, BUET, for providing me timely help, advice and necessary research facilities and taking care of my research work time to time.

I wish to express my gratitude to Dr. Md. Zakerullah, Prof. Department of Mathematics, BUET, for teaching me some special topics of fluid mechanics which helped me very much for my research and will also help me in future work and also for his encouragement about research.

I also express my gratitude to my colleagues Md. Abdul Maleque, Assistant Prof., and Md. Shakawat Hossain, lecturer, Department of Mathematics, Bangladesh University of Engineering & Technology for their cooperation and helps during my research work.

I am grateful to all my colleagues for their encouragement and helping mentally in all of works specially in my research work.

Abstract

The present dissertation deals with the problem of laminar natural convection around a horizontal cylinder. The external surface of this cylinder is everywhere isothermal, with the exception of a region, which is adiabatic. The effects of vertical cold walls are also determined.

The basic boundary layer equations have been reduced to local nonsimilarity equations. Solutions are obtained employing the perturbation method together with the Runge-Kutta initial value problem solver, the integral solution method and the finite volume method incorporating the SIMPLE algorithm on collocated body fitted grids.

Perturbation as well as finite volume solutions are obtained, respectively, for the leading edge and for the entire regimes. The results obtained are presented in terms of local heat transfer, streamlines, isothermal lines, velocity vectors, velocity and temperature profiles.

On analysing the heat transfer from the cylinder, it has been found that the intensity decreased and increased unexpectedly. The explanation can be given after visualization of flow. It is observed that the fluid near the vertical walls aspirated the layers of hot fluid from the horizontal cylinder. The uplift pressure and the tendency of the system to reach balance cause the fluid layers of the similar temperature and density to merge. However, this effect also found to be dependent on the intensity of the heat transfer.

Effects of the aforementioned physical quantities for fluid having different Grashof number and Prandtl number have been studied. The effects of the cold wall and adiabatic part of the cylinder on the flow and thermal fields have also been studied.

Nomenclature

C_p	specific heat at constant pressure
C_f	local skin friction
D	diameter of the cylinder
f	dimensionless stream function
g	acceleration due to gravity
Gr_x	local Grashof number
h	heat transfer coefficient
H_{Cyl}	height of the cylinder measured from the bottom of the wall
H_{wall}	wall height
k	thermal conductivity of the fluid
Nu_x	local Nusselt number
p	fluid pressure
Pr	Prandtl number
q_w	surface heat flux
Ra_r	Rayleigh number for the cylinder
Ra_x	Rayleigh number for walls
T	temperature in the boundary layer
T_w	temperature at the surface
T_∞	temperature of the ambient fluid
u, v	velocity components along x and y -directions respectively
W	width between the vertical walls
x, y	distance along & normal to the surface, respectively

Greek Letters

α	thermal diffusivity
β	coefficient of volumetric expansion
η	similarity variable
θ	dimensionless temperature
μ	kinematic coefficient of viscosity
ν	viscosity coefficient
ξ	local nonsimilarity variable
ρ	density of the fluid
τ_w	dimensionless shear stress
ϕ	inclination of the plate to the horizontal
ψ	stream function

List of figures

- Fig 1.1 Geometry of the problem
- Fig.2.1 The co-ordinate system
- Fig.3.1 Plot of the velocity profiles versus η for different values Pr
- Fig.3.2 Plot of the temperature profiles versus η for different values of Pr
- Fig.3.3 A typical Control Volume with different notations
- Fig. 3.4 Contour plot of streamlines for different wall spacing
- Fig 3.5 Change of Nusselt number for cylinder as width of walls function
- Fig 3.6 Contour plot of streamlines and Isotherms for $\varphi_w=60^\circ$
- Fig. 3.7 Plot of the u and v Velocity Profiles for $\varphi_w=60^\circ$
- Fig. 3.8 Plot of Isotherms for $\varphi_w=30^\circ$ and $Gr=10^4$
- Fig. 3.9 Plot of streamlines for $\varphi_w=30^\circ$ and $Gr=10^4$
- Fig. 3.10 Velocity vectors for $\varphi_w=30^\circ$ and $Gr=10^4$
- Fig. 3.11 Plot of the local Nusselt number distribution for $\varphi_w=30^\circ$ and $Gr=10^4$
- Fig. 3.12 Plot of the local Nusselt number distribution for $\varphi_w=90^\circ$ and $Gr=10^5$

Fig. 3.13 Plot of Isotherms for $\varphi_a=90^\circ$ and $Gr=10^5$

Fig 3.14 Plot of streamlines for $\varphi_a=90^\circ$ and $Gr=10^5$

Table 1 Effects of aspect ratio and height ratio on heat transfer intensity

Chapter 1



1.1 Introduction

Free convection around horizontal cylinders has been extensively investigated, both analytically and numerically, in the basic situation corresponding to a constant temperature of the surface. A little bit attention has so far been paid to other thermal conditions of noticeable practical interest, as are those relative to partly isothermal and partly adiabatic cylinders.

In engineering field, situations related to the last one that describe about practical problem; for example, in heat transfer around metallic tubes partially covered by snow or ice, or around pipes where an internal layer of deposited salt greatly decreases in some areas of the cylinders. Luciano [1], investigated the laminar free convection around horizontal cylinder. The author considered the cylinder surface partly isothermal and partly adiabatic. Cesini et. al. [2] studied the natural convection from horizontal cylinders in a rectangular cavity.

The study of heat transfer is of great interest in many branches of science and engineering. In the design of heat exchangers such as boilers, condensers, radiators, etc., for example, heat transfer analysis is essential for sizing such equipment. In the design of nuclear-reactor cores, a thorough heat transfer analysis of fuel elements is important for proper sizing of fuel elements to prevent burnout. In aerospace technology, heat transfer problems are crucial

because of weight limitations and safety considerations. In heating and air conditioning applications for buildings, a proper heat transfer analysis is necessary to estimate the amount of insulation needed to prevent excessive heat losses or gains.

The three distinct modes of heat transfer, namely conduction, convection and radiation must be considered. In reality, the combined effects of these three modes of heat transfer control temperature distribution in a medium. Conduction occurs if energy exchange takes place from the region of high temperature to that of low temperature by the kinetic motion or direct impact of molecules, as in the case of fluid at rest, and by the drift of electrons, as in the case of metals. The radiation energy emitted by a body is transmitted in the space in the form of electromagnetic waves. Energy is emitted from a material due to its temperature level, being larger for a larger temperature, and is then transmitted to another surface which may be vacuum or a medium which may absorb, reflect or transmit the radiation depending on the nature and extent of the medium. Considerable effort has been directed at the convective mode of heat transfer. In this mode, relative motion of the fluid provides an additional mechanism for energy transfer. A study of convective heat transfer involves the mechanisms of conduction and, sometimes, those of radiation processes as well. This makes the study of convective mode a very complicated one.

The convective heat transfer has been extensively investigated, both analytically and numerically, Bejan [6], Cebecci [9]. Kuhen [14] investigated experimentally the study of natural convection heat transfer in concentric and eccentric horizontal cylindrical annuli, Markin [16] studied the free convection boundary layers on cylinder of elliptic cross section, Convective heat transfer including natural convection has also been studied in [11-13] in different situations. The convective mode of heat transfer is divided into two basic processes. If the motion of the fluid arises due to an external agent such

as the externally imposed flow of a fluid over a heated object, the process is termed as forced convection. The fluid flow may be the result of a fan, a blower, the wind or the motion of the heated object itself. If the heat transfer to or from a body occurs due to an imposed flow of a fluid at a temperature different from that of the body, problems of forced convection encounters in technology. On the other hand, if the flow arises "naturally" simply due to the effect of a density difference, resulting from a temperature, in a body force field, such as gravitational field, the process is termed as natural or free convection. The density difference gives rise to buoyancy effects due to which the flow is generated. A heated body cooling in ambient air generates such a flow in the region surrounding it.

In many cases of practical interest forced and natural convection processes are important. Heat transfer by mixed convection is one in which neither forced convection nor natural convection is predominant. A heated body lying in still air loses energy by natural convection. But the body generates a buoyant flow above it. If another body is placed in that flow, the body is subjected to an external flow. Now it becomes essential to determine the natural as well as the forced convection effects and the region in which the heat transfer occurs.

Though natural convection process is much more complicated than that of forced convection, yet the study of natural convection process is also important because of the problem of heat rejection and removal in many devices, processes and systems. Natural convection represents a limit on the heat transfer rates and this becomes a very important consideration for problems in which other modes are either not possible or not practical. It is also relevant for safety consideration under conditions when the usual mode fails and the system has to depend on natural convection to get rid of the generated heat. To overheating such consideration in design are essential in many electronic devices and system and in power generation.

This study deals with the problem of laminar natural convection around a horizontal cylinder. The external surface of this cylinder is everywhere isothermal, with the exception of a region of variable extent, which is adiabatic, moreover this cylinder is placed within two vertical cold walls. The effects of cold walls on fluid flow and heat transfer will also be determined.

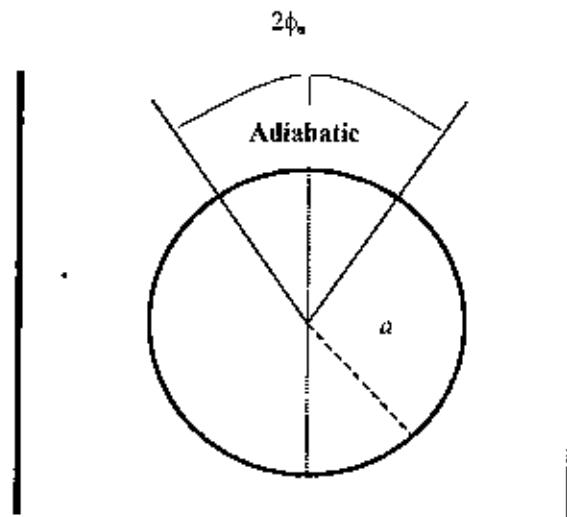


Fig.1.1 Geometry of the problem

Where in particular, the adiabatic sector corresponding to an angle $2\phi_a$ is symmetric with respect to the vertical diameter, whereas, the length of the relative arc is l , which could be reduced to zero in so restoring the fully isothermal situation.

The objective of the heat transfer analysis is the investigation of the Nusselt number distribution around the cylinder of different aspect ratios of the system

and at various Rayleigh numbers. The aspect ratio W^* is defined as $W^* = \frac{W}{D}$ where W is the width between the walls and D is the diameter of the cylinder.

In this study the equations governing the flow are reduced to non-similarity boundary layer equations. The derived non-similarity boundary layer equations are analysed using three distinct methods, namely, (i) Perturbation solution method together with the Runge-Kutta initial value problem solver for small ξ , a scaled streamwise co-ordinate, (ii) The integral solution method, and (iii) The finite volume method incorporating the SIMPLE algorithm on collocated body fitted grids

The resulting solutions have been presented in terms of local Nusselt number, streamlines, isotherms, velocity vectors, velocity and temperature profiles.

Effects of the aforementioned physical quantities for fluid having different Grashof numbers and Prandtl numbers have been studied. The effects of the cold walls and adiabatic part of the cylinder on the streamlines, isotherms, velocity vectors and local Nusselt number are also shown. Overall conclusions on the studies have also been given in this dissertation.

Chapter 2

2.1 MATHEMATICAL FORMULATIONS

The boundary-layer equations governing the flow are:

$$\frac{\partial u}{\partial x} + \frac{\partial v}{\partial y} = 0 \quad (2.1)$$

$$u \frac{\partial u}{\partial x} + v \frac{\partial u}{\partial y} = \nu \frac{\partial^2 u}{\partial y^2} \pm g\beta(T - T_\infty) \sin\left(\frac{x}{a}\right) \quad (2.2)$$

$$u \frac{\partial T}{\partial x} + v \frac{\partial T}{\partial y} = \alpha \frac{\partial^2 T}{\partial y^2} \quad (2.3)$$

with the boundary conditions

$$\begin{aligned} u = v = 0, T = T_w \quad ; y = 0 \\ T = T_w \text{ for isothermal part and } \frac{\partial T}{\partial y} = 0 \text{ for adiabatic part} \quad (2.4) \\ u = 0, T = T_\infty \text{ as } y \rightarrow \infty \end{aligned}$$

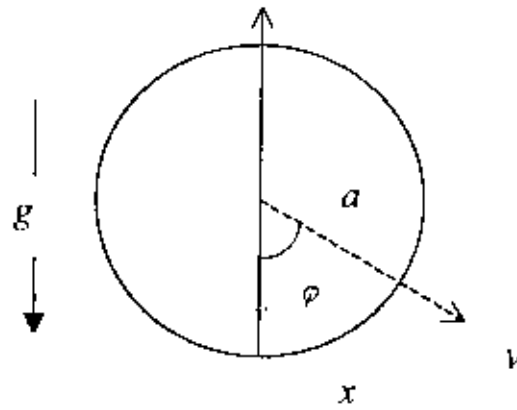


Fig.2.1: The co-ordinate system

The plus and minus signs in front of the buoyancy term in Eq. (2.2) apply, respectively, to flows due to heating and cooling. In writing the above equations, it is assumed that the fluid properties are constant except that the density variations within the fluid are allowed to contribute to the buoyancy forces. In the equations, u and v are, respectively, the velocity components in the x and y directions, T is the fluid temperature, ν is the kinematic viscosity, β is the thermal expansion coefficient, g is the acceleration due to gravity and T_∞ is the temperature of the ambient fluid.

2.2 TRANSFORMATION OF THE GOVERNING EQUATIONS

Now we introduce the following group of transformations of co-ordinates from (x,y) to (ξ, η) coordinates system in equations (2.1-2.3)

$$\eta = \frac{y}{a} Gr^{1/4}, \quad \xi = \frac{x}{a} \tag{2.5}$$

$$\psi(x, y) = \nu \xi Gr^{1/4} f(\xi, \eta) \tag{2.6}$$

20

$$\theta(\xi, \eta) = \frac{T(x, y) - T_\infty}{T_w - T_\infty} \quad (2.7)$$

where the stream function $\psi(x, y)$ satisfies the mass conservation equation with

$$u = \frac{\partial \psi}{\partial y}, v = -\frac{\partial \psi}{\partial x} \quad (2.8)$$

$$Gr = \frac{g\beta(T_w - T_\infty)}{\nu^2} a^3 \text{ is the Grashof number.} \quad (2.9)$$

$$\text{Also the Nusselt number, } Nu = \frac{Q_w a}{k(T_w - T_\infty)}$$

Here $\alpha > 0$ in equation (2.3) is for a heated cylinder in which case the buoyancy force term is positive and this aids the development of the boundary-layer (acting like a favorable pressure gradient), while $\alpha < 0$ represents the cooled cylinder and the buoyancy force opposes the development of the boundary layer.

Then the equations (2.2) to (2.3) transformed into (ξ, η) coordinate system as (The detailed calculations are in Appendix A)

$$f''' + ff'' - f'^2 + \frac{\sin \xi}{\xi} \theta = \xi \left(f' \frac{\partial f'}{\partial \xi} - f'' \frac{\partial f}{\partial \xi} \right) \quad (2.10)$$

$$\frac{1}{Pr} \theta'' + f\theta' = \xi \left(f' \frac{\partial \theta}{\partial \xi} - \theta' \frac{\partial f}{\partial \xi} \right) \quad (2.11)$$

where primes denote differentiation with respect to η and

$$\text{Prandtl number } Pr = \frac{\mu C_p}{k} = \frac{\nu}{\alpha}$$

The boundary conditions (2.4) become

$$f = \frac{\partial f}{\partial \eta} = 0, \quad \eta = 0$$

$$\theta = 1 \text{ (for isothermal part) and } \frac{\partial \theta}{\partial \eta} = 0 \text{ (for adiabatic part)}$$
(2.12)

$$\text{As } \eta \rightarrow \infty: \quad \frac{\partial f}{\partial \eta} = 0, \quad \theta = 0$$

In applications, quantities such as the surface rate of heat transfer Q_w and the shear stress or skin friction τ_w are very important. Here we present the results for these two items, which can be obtained in terms of the Nusselt number, Grashof number and the dimensionless frictional factor C_f . After obtaining velocity and temperature profiles, surface rate of heat transfer Q_w and skin friction τ_w can be calculated from the following relations:

$$Q = -k \left(\frac{\partial T}{\partial y} \right)_{y=0} = -k \frac{T_w - T_\infty}{a} Gr^{1/4} \theta'(\xi, 0)$$

and

$$\tau_w = \mu \left(\frac{\partial u}{\partial y} \right)_{y=0} = \frac{\rho \nu^2}{a^2} Gr^{3/4} \xi f''(0, \xi)$$
(2.13)

Thus we get

$$Nu Gr^{-1/4} = -\theta'(\xi, 0),$$

and

$$\frac{1}{2} C_f Gr^{-3/4} = \xi f''(\xi, 0)$$
(2.14)

Chapter 3

3 METHODS OF SOLUTIONS

In this section, three different methodologies, namely, (i) the perturbation method for small values of ξ , used by Hossain et. al. [3], Alim and Sadrul [8], (ii) the integral solution method used by Merk and Prins ($Pr \cong 1$) [10] and (iii) the finite volume method described by Ferziger [4] and Patankar [5] used by Mohamad [7] and H. Tasnim, S. Mahmud [15] are proposed to investigate the solutions of the equations governing the flow along a horizontal cylinder in vertical cold walls with partly adiabatic surface.

3.1 Perturbation solution (for small ξ)

The perturbation solution is valid for sufficiently small values of ξ . Accordingly the functions $f(\xi, \eta)$ and $\theta(\xi, \eta)$ are expanded in a power series in powers of ξ , that is, we assume

$$f(\xi, \eta) = \sum_{i=0}^{\infty} \xi^i f_i(\eta) \quad \text{and} \quad \theta(\xi, \eta) = \sum_{i=0}^{\infty} \xi^i \theta_i(\eta) \quad (3.1)$$

Substituting the above expansion into equations (2.10)-(2.11) and equating the coefficients of various powers of ξ we get the following equations:

(The detailed calculations are in Appendix B)

Basic set of equations $O(\xi^0)$:

$$f_0''' + f_0 f_0'' - f_0'^2 + \theta_0 = 0 \quad (3.2)$$

$$\frac{1}{Pr} \theta_0'' + f_0 \theta_0' = 0 \quad (3.3)$$

Where primes denote the derivatives with respect to η .

The corresponding boundary conditions are:

$$f_0 = f_0' = 0, \theta_0 = 1 \quad \text{at } \eta = 0 \quad \text{and} \quad f_0' = 0, \theta_0 = 0 \quad \text{as } \eta \rightarrow \infty$$

$$\text{for adiabatic part } \theta_0' = 0 \quad \text{as } \eta \rightarrow \infty \quad \text{and } \theta_0 \text{ is unknown} \quad (3.4)$$

First order perturbation equations $O(\xi^1)$:

$$f_1''' + (f_0 f_1'' + f_1 f_0'') - 2f_0' f_1' + \theta_1 = (f_0' f_1' - f_0'' f_1) \quad (3.5)$$

$$\frac{1}{Pr} \theta_1'' + (f_0 \theta_1' + f_1 \theta_0') = (f_0' \theta_1 - f_1 \theta_0') \quad (3.6)$$

The boundary conditions are:

$$f_1 = 0, f_1' = 0, \theta_1 = 0 \quad \text{at } \eta = 0 \quad \text{and} \quad f_1' = 0, \theta_1 = 0 \quad \text{as } \eta \rightarrow \infty \quad (3.7)$$

and for adiabatic part $\theta_1' = 0$ as $\eta \rightarrow \infty$ and θ_1 is unknown

Second order perturbation equations $O(\xi^2)$:

$$f_2''' + (f_0 f_2'' + f_1 f_1'' + f_2 f_0'') - (2f_0' f_2' + f_1' f_1') + (\theta_2 - \frac{\theta_0}{6}) \\ = \{2(f_0' f_2' - f_0'' f_2) + (f_1' f_1' - f_1'' f_1)\} \quad (3.8)$$

$$\frac{1}{Pr} \theta_2'' + (f_0 \theta_2' + f_1 \theta_1' + f_2 \theta_0') = \{2(f_0' \theta_2 - f_2 \theta_0') + (f_1' \theta_1 - f_1 \theta_1')\}$$

with the boundary conditions:

$$f_2 = f_2' = \theta_2 = 0 \quad \text{at } \eta = 0 \quad \text{and} \quad f_2' = \theta_2 = 0 \quad \text{as } \eta \rightarrow \infty$$

$$\text{and for adiabatic part } \theta_2' = 0 \quad \text{as } \eta \rightarrow \infty \quad \text{and } \theta_2 \text{ is unknown} \quad (3.9)$$

nth order perturbation equations $O(\xi^n)$:

$$f_n''' + \sum_{k=0}^n (1+k) f_k f_{n-k}'' - \sum_{k=0}^n (1+k) f_k' f_{n-k}' + \sum_{k=0}^{n/2} (-1)^k \frac{\theta_{n-2k}}{(2k+1)!} = 0 \quad (3.10)$$

$$\frac{1}{Pr} \theta_n'' + \sum_{k=0}^n (1+k) f_k \theta_{n-k}' - \sum_{k=0}^n k \theta_k f_{n-k}' = 0 \quad (3.11)$$

The boundary conditions are:

$$f_i = f_i' = \theta_i = 0 \quad \text{at } \eta = 0 \quad \text{and} \quad f_i' = \theta_i = 0 \quad \text{as } \eta \rightarrow \infty \\ \text{for } i = 2, 3, \dots, n \quad (3.12)$$

and for adiabatic part $\theta_i' = 0$ as $\eta \rightarrow \infty$ and θ_i is unknown

Zeroth order solutions:

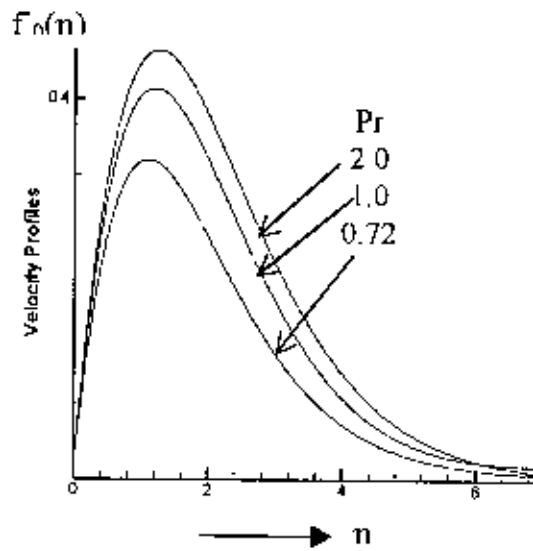


Fig. 3.1: Plot of the velocity profiles versus η for different values of Pr

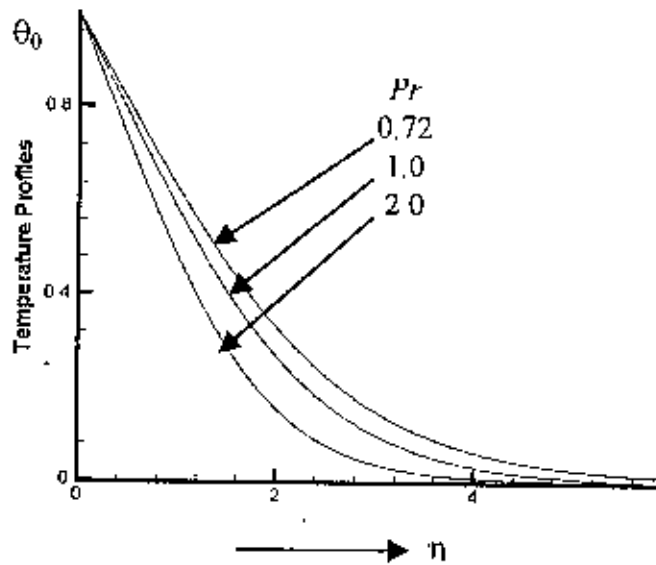


Fig. 3.2: Plot of the temperature profiles versus η for different values of Pr

3.2 Integral solution

An integral approach to the solution of the boundary-layer equations for the free convection around isothermal circular horizontal cylinders has been followed by several authors. In this study the integral form of the basic set of boundary-layer equations (2.2)-(2.3) together with boundary conditions (2.4) be solved by extending to the non-completely isothermal cases, the method used by Merk and Prins ($Pr \approx 1$) [10]

For the present case, a third degree polynomial is assumed for the velocity profile and a fifth degree polynomial for the dimensionless temperature profile. In particular taking into account the proper boundary conditions, we can put $\eta = \frac{y}{\delta}$ and

$$f = \frac{u\alpha}{\nu} = Gr^{1/2} F(\xi)\eta(1-\eta^2) \quad (3.13)$$

$$\theta = \frac{T - T_\infty}{T_w - T_\infty} = \theta_0 + \lambda\theta_1 \quad (3.14)$$

where

$$\begin{cases} \theta_0 = 1 - 10\eta^3 + 15\eta^4 - 6\eta^5 \\ \theta_1 = \eta - 6\eta^3 + 8\eta^4 - 3\eta^5 \end{cases} \quad (3.15)$$

and $\lambda = \left(\frac{d\theta}{d\eta}\right)_w$ is equal to zero on the adiabatic surface and is unknown along the isothermal surface.

$$\text{Taking into account that, at the wall, one has} \quad (3.16)$$

$$\left(\frac{d^3\theta}{d\eta^3}\right)_w = \left(\frac{du}{d\eta}\right)_w \left(\frac{d\theta}{d\xi}\right)_w$$

Then calculation yields $\lambda = -\frac{5}{3}$, Also $Nu = -\frac{\lambda}{\delta^*}$

where δ^* is boundary layer thickness dimensionless with respect to radius of the cylinder a

Introducing the new function $G(\xi) = Gr^{-1/4} / \delta^*(\xi)$, we have the differential equations for the isothermal region

$$\begin{aligned} \frac{dF}{d\varphi} &= \frac{35 \sin \varphi}{2 F} - \left(\frac{105}{2} + \frac{420}{17}\right) G^2, \\ \frac{dG}{d\varphi} &= \left[\frac{35 \sin \varphi}{2 F} - \left(\frac{105}{2} + \frac{2520}{21}\right) G^2 \right] \left(\frac{G}{F}\right) \end{aligned} \quad (3.17)$$

where for the angle φ the relation $\varphi = 2\xi$ holds. This system can be easily solved by simple numerical procedure like Runge-Kutta scheme or other methods, provided that the initial conditions at the forward stagnation point $\xi = 0$ are given. These conditions are obtained, following the same approach of [10], by matching the integral solutions to the similar solutions, F_s and G_s , around $\varphi=0$, that is

$$F_s = k_1 \varphi \quad \text{and} \quad G_s = k_2$$

In the present case, $k_1 = 2.060$ and $k_2 = 0.289$

Above the adiabatic part of the cylinder, the unknown functions are $F(\xi)$, $G(\xi)$ and θ_w . The integral equations and equation (3.17) provide

$$\frac{dF}{d\varphi} = \frac{105 \sin \varphi}{4 F} - \left(\frac{105}{2+30} \right) G^2 \quad (3.18)$$

$$\frac{dG}{d\varphi} = \left[\frac{105 \sin \varphi}{4 F} - \left(\frac{105}{2} + 60 \right) G^2 \right] \left(\frac{G}{F} \right) \quad (3.19)$$

$$\frac{dE}{d\varphi} = -30 \frac{EG^2}{F} \quad (3.20)$$

with the initial conditions $E(\varphi) = 1$, and $F(\varphi)$ and $G(\varphi)$ matching the solutions for the isothermal part of the cylinder.

3.3 Finite volume method

In the present study, the finite volume method has been used incorporating the SIMPLE algorithm. A control volume based finite volume method is used to discretize the governing equations. A body fitted grid with collocated variable arrangement is used.

Collocated scheme is efficient in the sense of computer memory saving, because pressure along with other variables is calculated at same location of grid. In this connection the CFD code called "CAFFA" has been modified for the present configuration and used to obtain the solutions for the problems. Present investigation was carried out for a range of orientation $0^\circ \leq \varphi_0 \leq 90^\circ$. Thermal field is presented in the form of isothermal lines. Heat transfer is presented graphically as well as in tabular form in Nusselt number for various Grashof numbers (Gr) and aspect ratios (W/D). Flow fields are presented in the form of streamlines, velocity vectors and also in velocity curves for different Grashof numbers and adiabatic part parameters φ_n .

NUMERICAL SCHEME

The primary variables are the Cartesian velocity components, pressure and temperature and the density is linked to temperature variation via Boussinesq approximation. Pressure-velocity coupling is achieved through SIMPLE algorithm. The discretization is carried out on control volumes defined by a boundary fitted, non-orthogonal grid. Since Cartesian base vectors are employed, the method is not sensitive to grid smoothness. The co-ordinate free integral forms

of the steady state conservation equations for mass, momentum and energy equations are as follows:

$$\int_S \rho \mathbf{v} \cdot \mathbf{n} dS = 0 \quad (3.1)$$

$$\int_S \rho u_i v_i \cdot \mathbf{n} dS = \int_S \mu \text{grad } u_i \cdot \mathbf{n} dS - \int_S p i_i \cdot \mathbf{n} dS + \int_V \rho g_i dV \quad (3.2)$$

$$\int_S \rho u_j v_j \cdot \mathbf{n} dS = \int_S \mu \text{grad } u_j \cdot \mathbf{n} dS - \int_S p i_j \cdot \mathbf{n} dS + \int_V \rho g_j dV \quad (3.3)$$

$$\int_S \rho T \mathbf{v} \cdot \mathbf{n} dS = \int_S \frac{\mu}{\text{Pr}} \text{grad } T \cdot \mathbf{n} dS \quad (3.4)$$

The Boussinesq approximation is:

$$\rho = \rho_0 [1 - \beta(T - T_0)] \quad (3.5)$$

The generalized form of equation (3.1) - (3.4) is given in equation (3.6)

$$\int_S \rho \phi \mathbf{v} \cdot \mathbf{n} dS = \int_S \Gamma \text{grad } \phi \cdot \mathbf{n} dS + \int_V q_\phi dV \quad (3.6)$$

Here, S is the surface and V is the volume of the arbitrary control volume, \mathbf{n} is the unit vector normal to S and directed outwards, \mathbf{v} is the velocity vector, u_i and u_j are the Cartesian velocity components, ρ is the density, μ is the viscosity, Pr is the Prandtl number, p and T are the pressure and temperature respectively.

DISCRETIZATION METHOD

The solution domain is subdivided into a finite number of contiguous quadrilateral control volumes (CV). The CVs are defined by coordinates of their vertices, which are assumed to be connected by straight lines. This simple form is possible due to the fact that the equations contain no curvature terms and only the projections of the CV faces onto Cartesian coordinate surfaces are required in the course of discretization, as demonstrated below. All the dependent variables solved for and all fluid properties are stored in the CV center (collocated arrangement). A suitable spatial distribution of dependent variables is assumed and the conservation equations (3.1) - (3.4) are applied to each CV, leading to a system of non-linear algebraic equations. The main steps of discretization procedure to calculate convection and diffusion fluxes and source terms are outlined below.

The mass flux through the cell face 'e' (Fig.3.2) is evaluated as:

$$\dot{m}_e = \int_{S_e} \rho \mathbf{V} \cdot d\mathbf{S} \approx (\rho \mathbf{V})_e \cdot \mathbf{S}_{1e} = \rho_e (U S_{1e}^x + V S_{1e}^y) \quad (3.7)$$

Where \mathbf{S}_{1e} is the surface vector representing the area of the cell face ($\xi = \text{const.}$) and S_{1e}^x and S_{1e}^y denotes its Cartesian components. These are given in terms of the CV vertex coordinates as follows:

$$S_{1e}^x = (y_n - y_s) \quad \text{and} \quad S_{1e}^y = -(x_n - x_s) \quad (3.8)$$

The mean cell face velocity components, U_e and V_e are obtained by interpolating neighbor nodal values in a way which ensures the stability of grid scheme. The convection flux of any variable ϕ can now be expressed as:

$$F_e^C = \int_{S_e} \rho \phi \mathbf{V} \cdot d\mathbf{S} \approx (\rho \phi \mathbf{V})_e \cdot \mathbf{S}_{1e} = \dot{m}_e \phi_e \quad (3.9)$$

The diffusion flux of ϕ is calculated as:

$$F_e^D = - \int_{S_e} \Gamma_\phi \text{grad } \phi \cdot d\mathbf{S} \approx - (\Gamma_\phi \text{grad } \phi)_e \cdot \mathbf{S}_{1e} \quad (3.10)$$

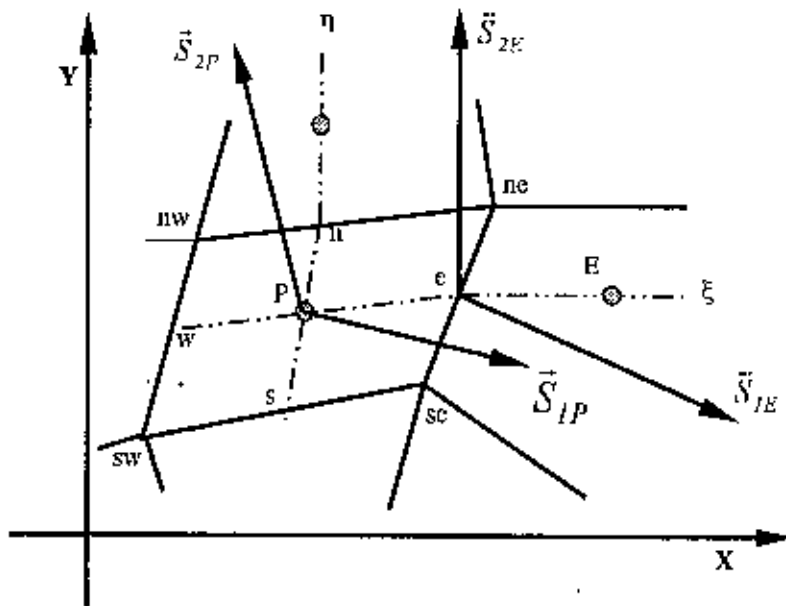


Fig.3.3 A typical CV with different notations

By expressing the gradient of ϕ at the cell face center 'e', which is taken here to represent the mean value over the whole cell face, through the derivatives in ξ and η directions (Fig.2) and by discretizing these derivatives with CDS, the following expression results:

$$F_e^D \approx \frac{\Gamma_{\phi, e}}{S_{1e} \cdot PE} \left[(\phi_E - \phi_P) (S_{1e} \cdot S_{1e}) + (\phi_n - \phi_s)_e (S_{2e} \cdot S_{2e}) \right] \quad (3.11)$$

PE is the vector representing the distance from P to E , directed towards E . S_{2e} is the surface vector orthogonal to PE and directed outwards positive η coordinate

(Fig 3 3), representing the area in the surface $\eta=0$ bounded by P and E. Its x and y components are:

$$S_{ze}^x = -(y_E - y_P) \quad \text{and} \quad S_{ze}^y = (x_E - x_P) \quad (3.12)$$

The volumetric source term is integrated by simply multiplying the specific source at the control volume center P (which is assumed to represent the mean value over the whole cell) with the cell volume i.e.

$$Q_\phi^v = \int_V q_\phi dV \approx (q_\phi)_P \Delta V \quad (3.13)$$

The pressure term in the momentum equations are treated as body force and may be regarded as pressure sources for the Cartesian velocity components. They are evaluated as:

$$Q_u^p = -\int_S p i_x dS = -\int_V (\text{grad } p \cdot i_x) dV \approx -[(p_e - p_w)S_{1e} + (p_n - p_s)S_{2e}] i_x \quad (3.14)$$

Where the surface vectors S_{1e} and S_{2e} represent the area of the CV cross section at $\xi=0$ and $\eta=0$ respectively. Since CV's are bounded by straight lines, these two vectors can be expressed through the CV surface vectors, e.g. $S_{1e}=0.5(S_{1e} + S_{1w})$. Terms in the momentum equations not featuring in equation (3.6) are discretized using the same approach and added to the source term.

After summing up all cell face fluxes and sources, the discretized transport equation reduces to the following algebraic equation

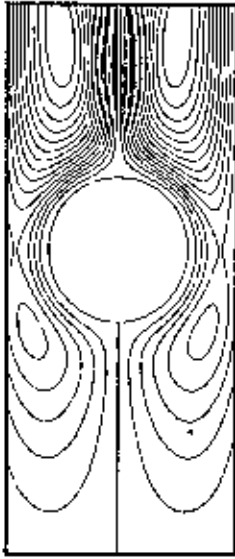
$$A_P \phi_P + \sum_{nb} A_{nb} \phi_{nb} = Q_\phi \quad (3.15)$$

Where the coefficients A_{nb} contains the convective and diffusive flux contributions and Q_ϕ represents the source term. The system of equations is solved by using Stone's SIP solver[4].

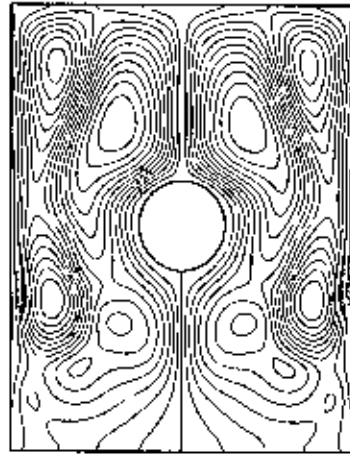
FLOW AND THERMAL FIELDS

At lower Grashof number, fluid near the cylinder wall is almost stagnant due to high viscous effect. Dominance of buoyant effect increases with the increase of Grashof number. Fluid motion is greatly affected by the orientation of the cylinder i.e. for different values of ϕ_a . Fluids are moving upwards along the cylinder surface creating the boundary layers and separates in some places due to the effects of adverse pressure gradient and adiabatic portion of the cylinder. As an effect of cold walls there is downward flow along the vertical walls. Fluid velocity is zero at the wall and at the tip of the boundary layer. In between wall and boundary layers, velocity is the maximum and thus depends on Grashof number.

Isothermal lines are presented in the Figures for some values of adiabatic part parameter ϕ_a , different aspect ratios and different Grashof numbers (Gr) and different Rayleigh numbers (Ra). Upward velocity is almost negligible for high viscous force. Buoyant force starts to dominate with the increase of Grashof number. Isothermal lines are concentrated near the cylinder wall showing high temperature gradient as well as high heat transfer. There are separation points in the thermal boundary layers in different positions due to the effect of adiabatic part of the cylinder



(a) $W/D = 1.3$



(b) $W/D = 4.0$

Fig. 3.4: Contour plot of streamlines for different wall spacing

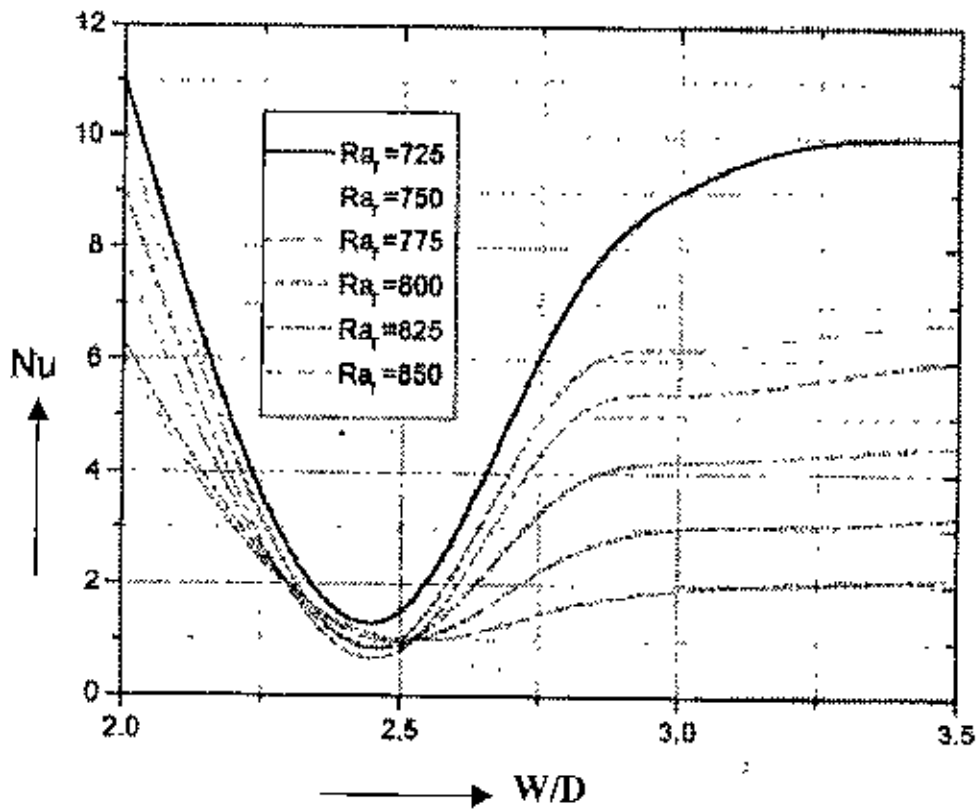
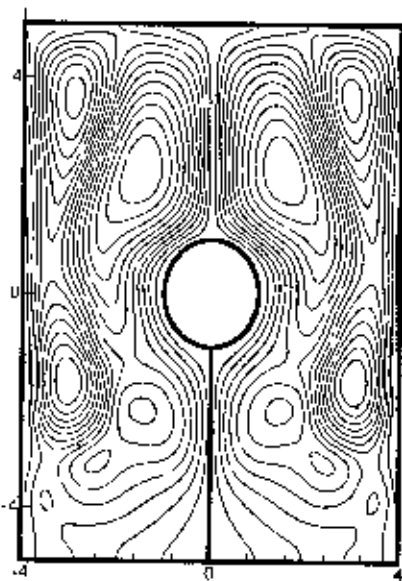
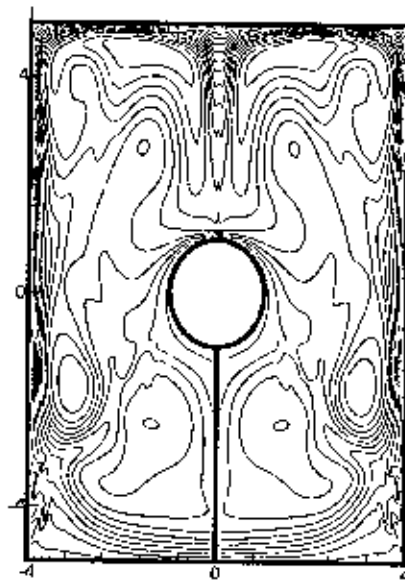


Fig. 3.5. Change of Nusselt number for cylinder as width of walls function



Streamlines



Isotherms

Fig. 3.6: Contour plot of streamlines and Isotherms for $\varphi_a=60^\circ$

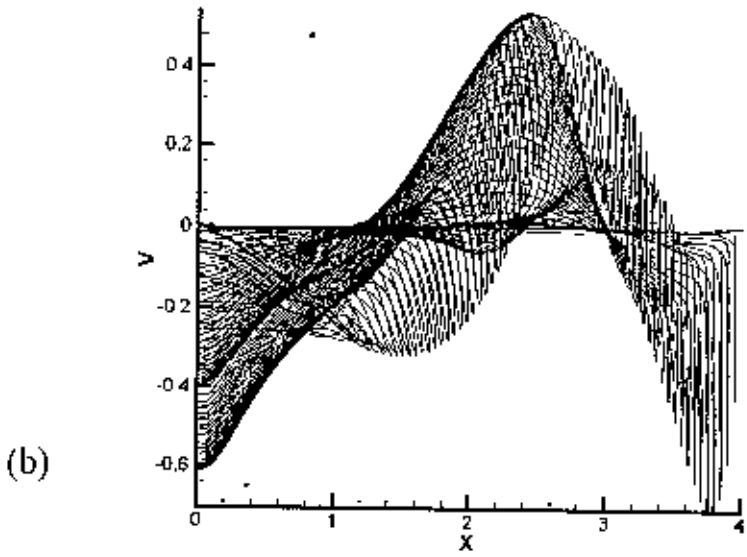
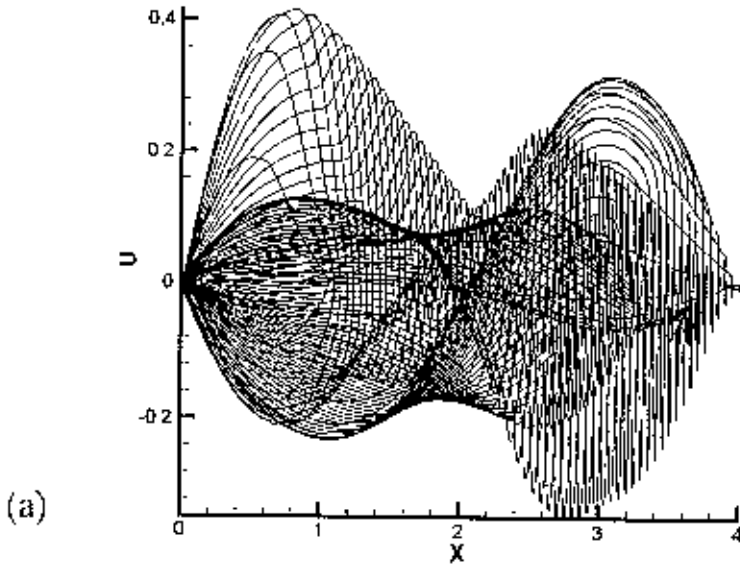


Fig. 3.7: Plot of the u and v Velocity Profiles for $\phi_a=60^\circ$

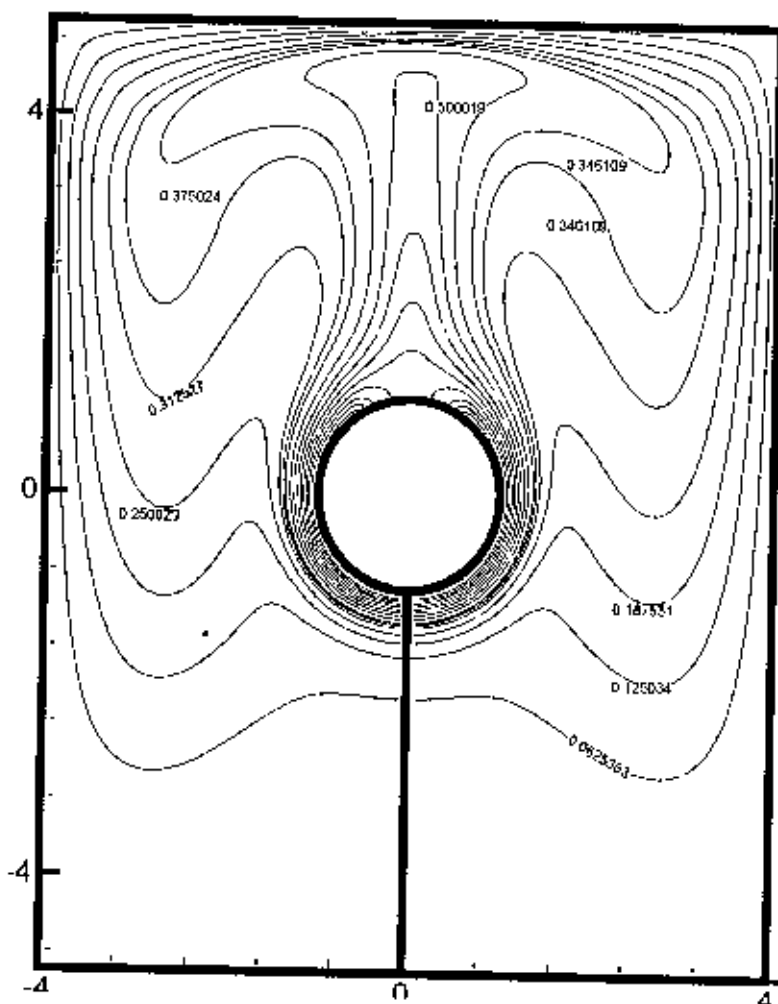


Fig. 3.8: Plot of Isotherms for $\phi_a=30^\circ$ and $Gr=10^4$

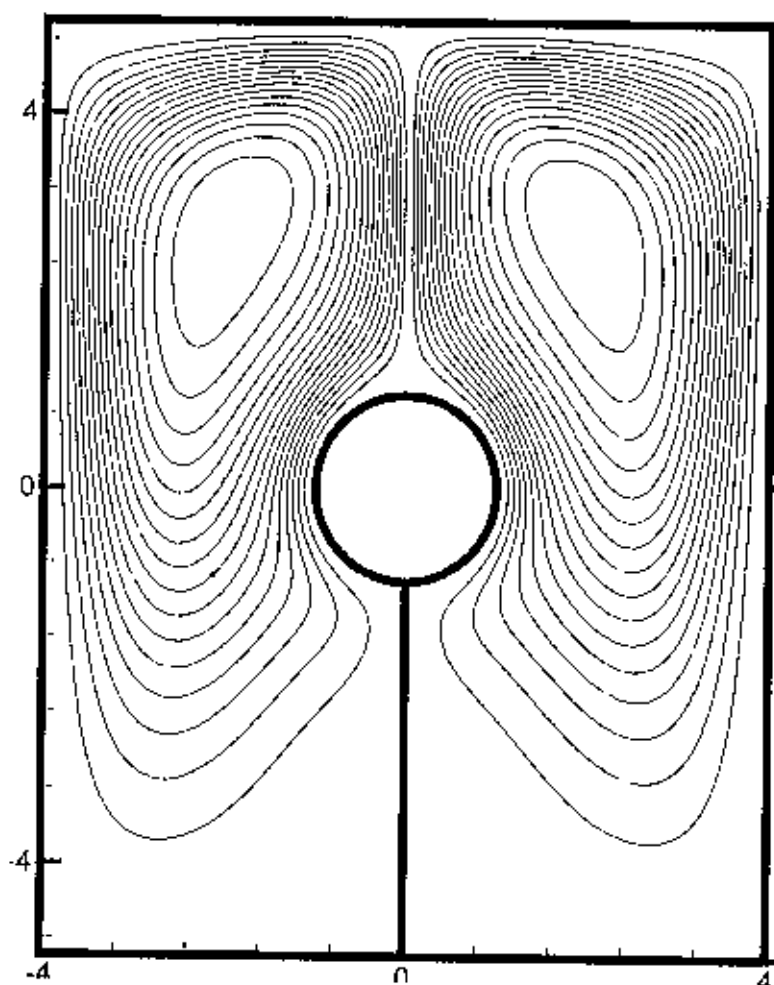


Fig. 3.9: Plot of streamlines for $\varphi_a=30^\circ$ and $Gr=10^4$

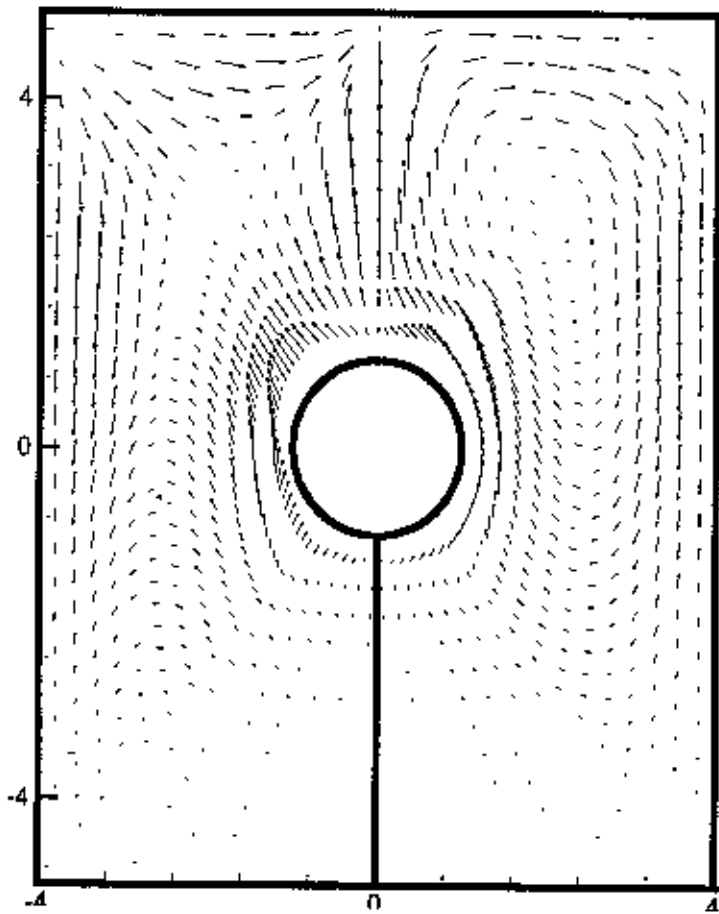


Fig. 3.10: Velocity vectors for $\phi_a=30^\circ$ and $Gr=10^4$

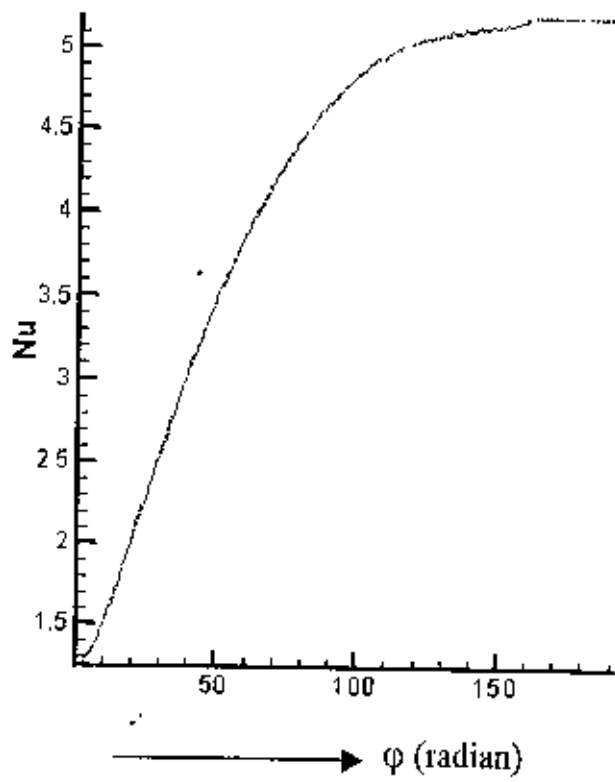


Fig. 3.11: Plot of the local Nusselt number distribution for $\phi_a=30^\circ$ and $Gr=10^4$

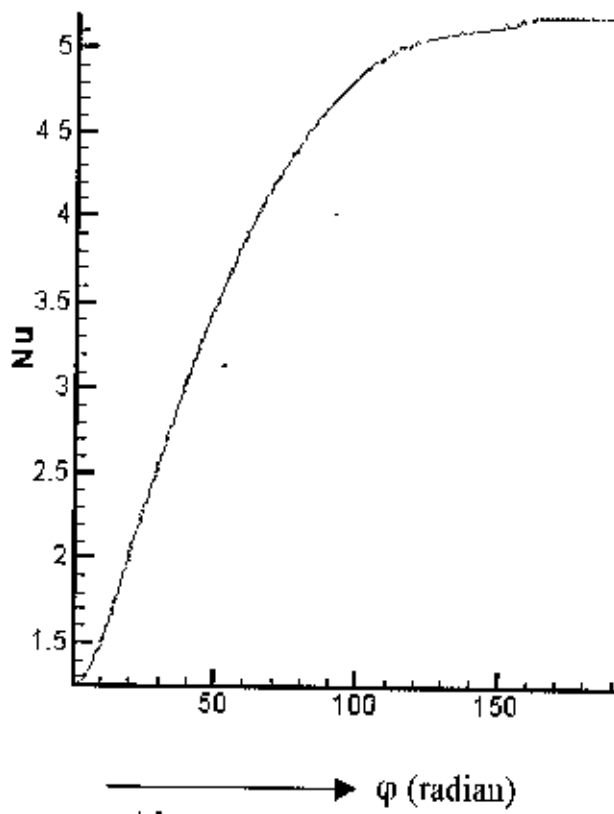


Fig. 3.12: Plot of the local Nusselt number distribution for $\varphi_a=90^\circ$ and $Gr=10^5$

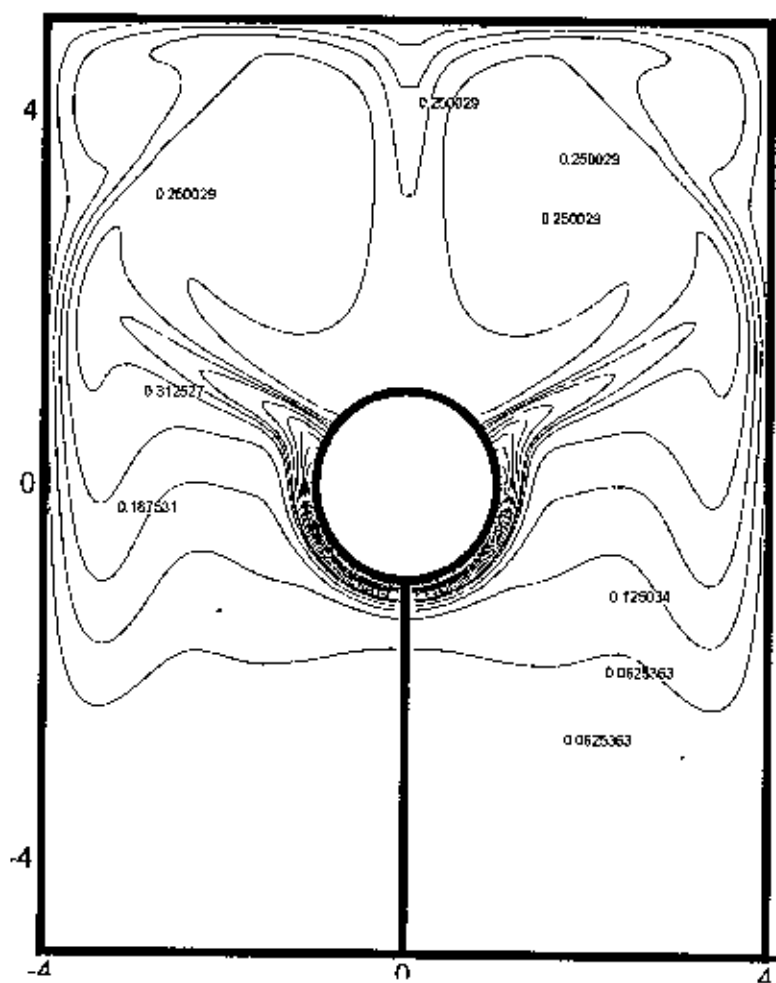


Fig. 3.13: Plot of Isotherms for $\phi_a=90^\circ$ and $Gr=10^5$

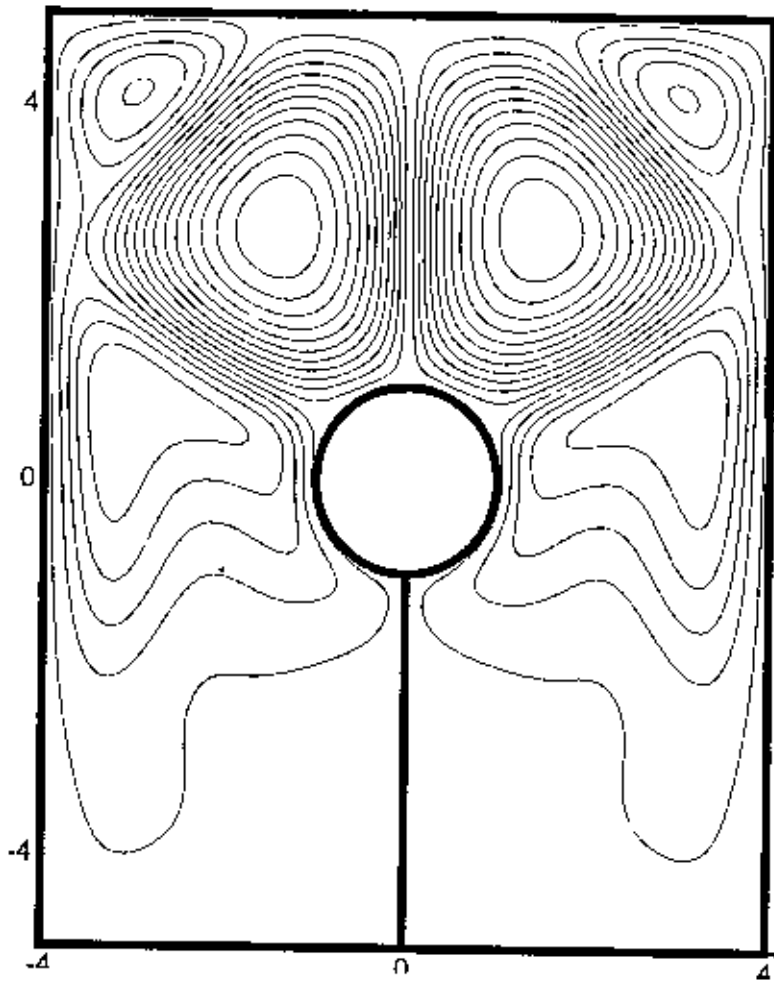


Fig. 3.14: Plot of streamlines for $\varphi_0=90^\circ$ and $Gr=10^5$

Table 1. Effects of aspect ratio and height ratio on heat transfer intensity

Aspect ratio W/D	Height ratio H_{cvl} / H_{wall}	Surface heat transfer Q_w
2.0	0.05	11.16
2.0	0.16	12.68
2.0	0.33	12.72
2.5	0.16	11.44
2.5	0.33	11.25
3.3	0.05	11.37
3.3	0.33	12.75
5.0	0.05	12.29

Results and discussions

The natural convection investigation performed on horizontal cylinder placed between isothermal vertical, parallel walls indicate that decrease in intensity of heat transfer, approximating the value of $W/D=2.5$ coefficient, where maximum heat transfer coefficient for all investigated cases was observed. The increase in heat transfer intensity for W/D below minimum heat transfer coefficient results from the increasing influence of diffusion flow over the convection. The most effective transfer takes place at coefficient value approximately 3.5. The shape of curves (Fig 3.5) obtained in this investigation remains in accordance with the shape of the curve presented by Naylor and Tarasuk [17] for a vertical plate placed in vertical walls. The qualitative investigation of this phenomena confirm the fact of change in the character of the fluid between the walls for such small width of the walls.

Fig. 3.1 shows the velocity profile against η for different values of Pr. It shows that the velocity decreases with Pr. Fig. 3.2 shows the temperature profiles against η for different values of Pr. It is evident that near the surface the velocity becomes zero, then increases, becomes maximum, then decreases and finally takes asymptotic value. It is obtained from the figure that the temperature decreases with increasing Pr. Fig 3.4 shows the Contour plot of streamlines for different position of vertical side walls i.e. for different aspect ratio ($W/D=1.3$ and 4.0). The effects of wall spacing in the flow fields are clearly shown in the figures.

Fig. 3.6 shows the Contour plot of streamlines and isotherms for $\phi_a=60^\circ$. We can observe from the figures that the effects of vertical walls on thermal fields are more significant than that of flow fields. The most important phenomenon observed during the investigations is the structure of the flow around the cylinder

placed inside the walls as it can be seen in the figures, hot fluid layers near hot elements are 'glued' to each other. Thus, we can suppose that this effect of joining of the layers will result in local increase of the flow speed. The effect of 'joining' of fluid layers is most visible for the width of the walls for which the increase in heat transfer was stated after quantitative measurements.

Some typical velocity curves are shown in Fig.3.7. There are u and v Velocity curves for $\varphi_a=60^\circ$ in different figures (a) and (b) respectively. Nothing special in the velocity curves actually. Many velocity curves over the region are shown in a figure just to show that the velocity profiles in this investigation are same as the usual velocity profiles.

Fig.3.8 and Fig.3.13 represent fields of temperature around horizontal cylinder within the walls, which was placed on high ratio $H_{cyl}/H_{wall}=0.4$. In the pictures it was shown how the temperature field was changed according to increase of adiabatic part and Grashof number. The adiabatic coefficient φ_a from 30° to 90° and Gr from 10^4 to 10^5 . Point of separation in thermal boundary layer is faster if the coefficient increases in the case of increment of adiabatic part.

In Fig.3.9 and Fig 3 14 we can observe the flow fields for $\varphi_a=30^\circ$, $Gr=10^4$ and $\varphi_a=90^\circ$, $Gr=10^5$. The change in flow field according to increase φ_a and Gr have been shown in the figures. The transition of single cell flow in each side of cylinder to the multi-cellular flow occurs due to the increase of Gr and φ_a .

Fig.3.10 shows the vector field of velocity for $\varphi_a=30^\circ$ and $Gr=10^4$. We observe that the maximum velocity occurs in the upper region of the cylinder. Fluid velocity is upward near the cylinder surface and downward along the vertical walls as an effect of their low temperature. For these kinds of forward and backward flows vorticity develops in some regions of the flow field.

In Fig.3.11 and Fig.3.12 the local Nusselt number distribution against the φ coordinate for the adiabatic parameter $\varphi_a=30^\circ$, $Gr=10^4$ and $\varphi_a=90^\circ$, $Gr=10^5$ presented respectively. We could not find any significant change in these curves due to φ_a and Gr but there are great increment in Nu with the φ coordinate.

The influence of width of the wall on heat transfer intensity has been presented in Table 1. For width coefficient $W/D < 2.0$ the heat transfer proceeded mainly by diffusion stream. The hot stream layer from the cylinder is strongly 'glued' to fluid layer from the wall. In this case the convection movement cannot develop.

Conclusions

Effects of confining cold walls on the free convection from a horizontal cylinder are studied analytically, and numerically for the various Grashof and Prandtl numbers considered, an optimum wall to wall spacing was obtained for the maximum rate of heat transfer from the cylinder. Some part of the cylinder is considered adiabatic and the effects of change in adiabatic part also determined.

Perturbation as well as finite volume solutions are obtained, respectively, for the leading edge and for the entire regimes. The results obtained are presented in terms of local Nusselt numbers, streamlines, Isothermal lines, velocity profiles and velocity vectors.

We observed from the investigations that at lower Grashof number, fluid near the cylinder wall is almost stagnant due to high viscous effect. Dominance of buoyant effect increases with the increase of Grashof number. Fluid motion is affected by the adiabatic part of the cylinder and by the cold walls. From the leading edge, fluids are moving upwards along the two vertical walls. Fluid velocity is zero at the wall and at the tip of the boundary layer. In between the walls and boundary layer, velocity is the maximum and this depends on Grashof number. Upward

velocity is almost negligible for high viscous force. Buoyant force starts to dominate with the increase of Grashof number. Isothermal lines are concentrated near the cylinder surface showing high temperature gradient as well as high heat transfer.

Summing the obtained results we may state that:

1. For each wall the entry region fragment (reaching the height $H_{cy}/H_{wall}=0.2$), where temperature stabilisation takes place, is identified. The influence of height at which the horizontal cylinder is placed (where the width of the walls is insignificant) determines the temperature on the cylinder. It is necessary to define the so-called inflow temperature in the analysis of the problem, because geometrical position of the cylinder and the slot affects the structure of the flow.
2. For the ratio $W/D < 2.0$, dominating impact of heat transfer is detected. In such case convection movements from horizontal cylinder are inhibited by the cold walls. The increase of this ratio above the quoted value causes a decrease in diffusion intensity, and development of convection.
3. The optimal value of heat transfer intensity is obtained for the horizontal cylinder, placed between two isothermal walls, for W/D ratio between 3.0 and 5.0.
4. The effect of 'gluing' of the layers is characteristic of the range in which the optimal heat transfer intensity takes place.
5. The effects of cold walls cause the downward flow and creation vorticity and flow cells in the flow region. Also the separation in boundary layers faster in the case of increment of adiabatic part.

Appendix A

Transformation of momentum and energy equations

The continuity, momentum and energy equations are:

$$\frac{\partial u}{\partial x} + \frac{\partial v}{\partial y} = 0 \quad (\text{A1})$$

$$u \frac{\partial u}{\partial x} + v \frac{\partial u}{\partial y} = \nu \frac{\partial^2 u}{\partial y^2} \pm g\beta(T - T_\infty) \sin\left(\frac{x}{a}\right) \quad (\text{A2})$$

$$u \frac{\partial T}{\partial x} + v \frac{\partial T}{\partial y} = \alpha \frac{\partial^2 T}{\partial y^2} \quad (\text{A3})$$

As $u = \frac{\partial \psi}{\partial y}$ and $v = -\frac{\partial \psi}{\partial x}$,

the stream function $\psi(x, y) = \nu \xi Gr^{1/4} f(\xi, \eta)$ automatically satisfies the mass conservation equation (A1). Now to get the corresponding transformed equations of momentum and energy equations (A2) and (A3) we have to follow the calculation below

$$\eta = \frac{y}{a} Gr^{1/4} \text{ and } \xi = \frac{x}{a}, \quad Gr = \frac{g\beta(T_w - T_\infty)}{\nu^2} a^3$$

$$\text{So } \frac{\partial \eta}{\partial y} = \frac{Gr^{1/4}}{a} = \frac{\eta}{y} \text{ and } \frac{\partial \xi}{\partial x} = \frac{1}{a} = \frac{\xi}{x}$$

Now from $\psi(x, y) = \nu \xi Gr^{1/4} f(\xi, \eta)$ we get

$$\begin{aligned} u = \frac{\partial \psi}{\partial y} &= \nu \xi Gr^{1/4} \frac{\partial f(\xi, \eta)}{\partial \eta} \left(\frac{Gr^{1/4}}{a} \right) \\ &= \frac{\nu \xi Gr^{1/2}}{a} f'(\xi, \eta) \end{aligned} \quad \text{where } f'(\xi, \eta) = \frac{\partial f(\xi, \eta)}{\partial \eta}$$

$$\begin{aligned} v = -\frac{\partial \psi}{\partial x} &= -\nu Gr^{1/4} \left(\frac{1}{a} f(\xi, \eta) + \xi \frac{\partial f}{\partial \xi} \frac{1}{a} \right) \\ &= -\frac{\nu Gr^{1/4}}{a} \left(f(\xi, \eta) + \xi \frac{\partial f}{\partial \xi} \right) \end{aligned}$$

$$\frac{\partial u}{\partial y} = \frac{\nu \xi Gr^{3/4}}{a^2} f''(\xi, \eta) \quad \text{and} \quad \frac{\partial^2 u}{\partial y^2} = \frac{\nu \xi Gr}{a^3} f'''(\xi, \eta)$$

$$\frac{\partial u}{\partial x} = \frac{\nu Gr^{1/2}}{a^2} \left(f'(\xi, \eta) + \xi \frac{\partial f'}{\partial \xi} \right)$$

$$\theta(\xi, \eta) = \frac{T(x, y) - T_\infty}{T_w - T_\infty} \quad \text{Therefore } T - T_\infty = (T_w - T_\infty) \theta(\xi, \eta)$$

Now

$$u \frac{\partial u}{\partial x} = \nu^2 \xi \frac{Gr}{a^3} \left(f'^2 + \xi f' \frac{\partial f'}{\partial \xi} \right)$$

$$\nu \frac{\partial u}{\partial x} = -\nu^2 \xi \frac{Gr}{a^3} \left(ff'' + \xi f'' \frac{\partial f}{\partial \xi} \right)$$

$$\nu \frac{\partial^2 u}{\partial y^2} = \nu^2 \xi \frac{Gr}{a^3} f'''(\xi, \eta)$$

$$g\beta(T - T_\infty) \sin\left(\frac{x}{a}\right) = g\beta(T_w - T_\infty) \theta \sin \xi$$

Substituting the above results in the momentum equation (A2) and dividing all

the terms by the factor $\nu^2 \xi \frac{Gr}{a^3}$ we get

$$f'^2 + \xi f' \frac{\partial f'}{\partial \xi} - ff'' - \xi f'' \frac{\partial f}{\partial \xi} = f''' + \frac{g\beta(T_w - T_\infty) a^3 \sin \xi}{\nu^2 Gr \xi}$$

Which implies

$$f''' + ff'' - f'^2 + \frac{\sin \xi}{\xi} \theta = \xi \left(f' \frac{\partial f'}{\partial \xi} - f'' \frac{\partial f}{\partial \xi} \right)$$

This is the momentum equation in non-dimensional form

Similarly for energy equation we have to perform the following calculation

$$T - T_\infty = \Delta T \theta(\xi, \eta) \quad \text{where } \Delta T = T_w - T_\infty$$

$$\frac{\partial T}{\partial y} = \Delta T \frac{\partial \theta(\xi, \eta)}{\partial \eta} \left(\frac{Gr^{1/4}}{a} \right) = (\Delta T) \frac{Gr^{1/4}}{a} \theta'(\xi, \eta)$$

$$\frac{\partial^2 T}{\partial y^2} = (\Delta T) \frac{Gr^{1/2}}{a^2} \theta''(\xi, \eta)$$

$$\frac{\partial T}{\partial x} = \Delta T \frac{\partial \theta}{\partial \xi} \frac{\partial \xi}{\partial x} = (\Delta T) \frac{1}{a} \frac{\partial \theta}{\partial \xi}$$

Now

$$u \frac{\partial T}{\partial x} = v \xi \frac{Gr^{1/2}}{a^2} \Delta T \frac{\partial \theta}{\partial \xi} f'$$

$$v \frac{\partial T}{\partial y} = -\frac{v Gr^{1/2}}{a^2} \Delta T \left(f \theta' + \xi \theta'' \frac{\partial f}{\partial \xi} \right)$$

$$\alpha \frac{\partial^2 T}{\partial y^2} = \alpha(\Delta T) \frac{Gr^{1/2}}{a^2} \theta''(\xi, \eta)$$

Substituting the above results in the energy equation (A3) and dividing all the terms by the factor $\frac{\nu(\Delta T)Gr^{1/2}}{\alpha^2}$

we get

$$\xi \left(f' \frac{\partial \theta}{\partial \xi} \right) - f\theta' - \xi \left(\theta' \frac{\partial f}{\partial \xi} \right) = \frac{\alpha}{\nu} \theta''$$

So

$$\frac{1}{Pr} \theta'' + f\theta' = \xi \left(f' \frac{\partial \theta}{\partial \xi} - \theta' \frac{\partial f}{\partial \xi} \right)$$

Which is the energy equation in dimensionless form.

Appendix B

Details of the perturbation equations

The transformed momentum and energy equations are:

$$f''' + ff'' - f'^2 + \frac{\sin \xi}{\xi} \theta = \xi \left(f' \frac{\partial f'}{\partial \xi} - f'' \frac{\partial f}{\partial \xi} \right)$$

$$\frac{1}{Pr} \theta'' + f\theta' = \xi \left(f' \frac{\partial \theta}{\partial \xi} - \theta' \frac{\partial f}{\partial \xi} \right)$$

To get the perturbation equations of various orders we assume

$$f(\xi, \eta) = \sum_{i=0}^{\infty} \xi^i f_i(\eta) \quad \text{and} \quad \theta(\xi, \eta) = \sum_{i=0}^{\infty} \xi^i \theta_i(\eta)$$

i.e.

$$f(\xi, \eta) = f_0(\eta) + \xi^1 f_1(\eta) + \xi^2 f_2(\eta) + \xi^3 f_3(\eta) + \dots$$

$$\theta(\xi, \eta) = \theta_0(\eta) + \xi^1 \theta_1(\eta) + \xi^2 \theta_2(\eta) + \xi^3 \theta_3(\eta) + \dots$$

or

$$f'(\xi, \eta) = f'_0(\eta) + \xi^1 f'_1(\eta) + \xi^2 f'_2(\eta) + \xi^3 f'_3(\eta) + \dots$$

$$f''(\xi, \eta) = f''_0(\eta) + \xi^1 f''_1(\eta) + \xi^2 f''_2(\eta) + \xi^3 f''_3(\eta) + \dots$$

$$\frac{\partial f(\xi, \eta)}{\partial \xi} = f_1(\eta) + 2\xi f_2(\eta) + 3\xi^2 f_3(\eta) + \dots$$

Similarly

$$\theta''(\xi, \eta) = \theta_0''(\eta) + \xi^1 \theta_1''(\eta) + \xi^2 \theta_2''(\eta) + \xi^3 \theta_3''(\eta) + \dots$$

$$\frac{\partial \theta(\xi, \eta)}{\partial \xi} = \theta_1(\eta) + 2\xi \theta_2(\eta) + 3\xi^2 \theta_3(\eta) + \dots$$

(1) Substituting the corresponding terms into momentum equation

$$f''' + ff'' - f'^2 + \frac{\sin \xi}{\xi} \theta = \xi \left(f' \frac{\partial f'}{\partial \xi} - f'' \frac{\partial f}{\partial \xi} \right)$$

we get,

$$\begin{aligned} & \left(f_0''(\eta) + \xi^1 f_1''(\eta) + \xi^2 f_2''(\eta) + \xi^3 f_3''(\eta) + \dots \right) + \\ & \left(f_0(\eta) + \xi^1 f_1(\eta) + \xi^2 f_2(\eta) + \xi^3 f_3(\eta) + \dots \right) \left(f_0''(\eta) + \xi^1 f_1''(\eta) + \xi^2 f_2''(\eta) + \xi^3 f_3''(\eta) + \dots \right) \\ & + \left(1 - \frac{\xi^2}{3!} + \frac{\xi^4}{5!} - \frac{\xi^6}{7!} + \frac{\xi^8}{9!} - \dots \right) \left(\theta_0(\eta) + \xi^1 \theta_1(\eta) + \xi^2 \theta_2(\eta) + \dots \right) \\ & = \xi \left[\left(f_0'(\eta) + \xi^1 f_1'(\eta) + \xi^2 f_2'(\eta) + \xi^3 f_3'(\eta) + \dots \right) \left(f_1'(\eta) + 2\xi f_2'(\eta) + 3\xi^2 f_3'(\eta) + \dots \right) \right. \\ & \quad \left. - \left(f_0''(\eta) + \xi^1 f_1''(\eta) + \xi^2 f_2''(\eta) + \xi^3 f_3''(\eta) + \dots \right) \left(f_1(\eta) + 2\xi f_2(\eta) + 3\xi^2 f_3(\eta) + \dots \right) \right] \end{aligned}$$

Sorting the similar powers of ξ and rewriting the above equations we get,

$$\begin{aligned}
& (f_0''' + f_0 f_0'' - f_0'^2 + \theta_0) + \{f_1''' + (f_0 f_1'' + f_1 f_0'') - 2f_0' f_1' + \theta_1 - (f_0' f_1' - f_0'' f_1)\} \xi \\
& + \left\{ f_2''' + (f_0 f_2'' + f_1 f_1'' + f_2 f_0'') - (2f_0' f_2' + f_1' f_1') + (\theta_2 - \frac{\theta_0}{6}) \right. \\
& \quad \left. - \{2(f_0' f_2' - f_0'' f_2) + (f_1' f_1' - f_1'' f_1)\} \right\} \xi^2 + \dots \\
& \dots + \left\{ f_n''' + \sum_{k=0}^n (1+k) f_k f_{n-k}'' - \sum_{k=0}^n (1+k) f_k' f_{n-k}' + \sum_{k=0}^{n/2} (-1)^k \frac{\theta_{n-2k}}{(2k+1)!} \right\} \xi^n + \dots = 0
\end{aligned}$$

Then equating the coefficients of various powers of ξ we can get the perturbation equations of any order. Here the equations for $\xi^0, \xi^1, \xi^2, \xi^n$ have been presented:

$$f_0''' + f_0 f_0'' - f_0'^2 + \theta_0 = 0$$

$$f_1''' + (f_0 f_1'' + f_1 f_0'') - 2f_0' f_1' + \theta_1 = (f_0' f_1' - f_0'' f_1)$$

$$\begin{aligned}
f_2''' + (f_0 f_2'' + f_1 f_1'' + f_2 f_0'') - (2f_0' f_2' + f_1' f_1') + (\theta_2 - \frac{\theta_0}{6}) \\
= \{2(f_0' f_2' - f_0'' f_2) + (f_1' f_1' - f_1'' f_1)\}
\end{aligned}$$

$$f_n''' + \sum_{k=0}^n (1+k) f_k f_{n-k}'' - \sum_{k=0}^n (1+k) f_k' f_{n-k}' + \sum_{k=0}^{n/2} (-1)^k \frac{\theta_{n-2k}}{(2k+1)!} = 0$$

(2) Similarly substituting the corresponding terms into energy equation

$$\frac{1}{Pr}\theta'' + f\theta' = \xi \left(f' \frac{\partial \theta}{\partial \xi} - \theta' \frac{\partial f}{\partial \xi} \right)$$

we get,

$$\begin{aligned} & \frac{1}{Pr} (\theta_0''(\eta) + \xi^1 \theta_1''(\eta) + \xi^2 \theta_2''(\eta) + \xi^3 \theta_3''(\eta) + \dots) \\ & (f_0(\eta) + \xi^1 f_1(\eta) + \xi^2 f_2(\eta) + \xi^3 f_3(\eta) + \dots) (\theta_0'(\eta) + \xi^1 \theta_1'(\eta) + \xi^2 \theta_2'(\eta) + \dots) \\ & = \xi \left[(f_0'(\eta) + \xi^1 f_1'(\eta) + \xi^2 f_2'(\eta) + \xi^3 f_3'(\eta) + \dots) (\theta_1(\eta) + 2\xi \theta_2(\eta) + 3\xi^2 \theta_3(\eta) + \dots) \right. \\ & \quad \left. - (\theta_0'(\eta) + \xi^1 \theta_1'(\eta) + \xi^2 \theta_2'(\eta) + \dots) (f_1(\eta) + 2\xi f_2(\eta) + 3\xi^2 f_3(\eta) + \dots) \right] \end{aligned}$$

Rewriting the above equations we get,

$$\begin{aligned} & \left(\frac{1}{Pr} \theta_0'' + f_0 \theta_0' \right) + \left\{ \frac{1}{Pr} \theta_1'' + (f_0 \theta_1' + f_1 \theta_0') - (f_0' \theta_1 - f_1 \theta_0') \right\} \xi \\ & + \left\{ \frac{1}{Pr} \theta_2'' + (f_0 \theta_2' + f_1 \theta_1' + f_2 \theta_0') - \{ 2(f_0' \theta_2 - f_2 \theta_0') + (f_1 \theta_1' - f_1' \theta_1) \} \right\} \xi^2 + \dots \\ & \dots + \left\{ \frac{1}{Pr} \theta_n'' + \sum_{k=0}^n (1+k) f_k \theta_{n-k}' - \sum_{k=0}^n k \theta_k f_{n-k}' \right\} \xi^n + \dots = 0 \end{aligned}$$

Then equating the coefficients of $\xi^0, \xi^1, \xi^2, \xi^n$ we get the following perturbation equations:

$$\frac{1}{\text{Pr}} \theta_0'' + f_0 \theta_0' = 0$$

$$\frac{1}{\text{Pr}} \theta_1'' + (f_0 \theta_1' + f_1 \theta_0') = (f_0' \theta_1 - f_1 \theta_0')$$

$$\frac{1}{\text{Pr}} \theta_2'' + (f_0 \theta_2' + f_1 \theta_1' + f_2 \theta_0') = \{2(f_0' \theta_2 - f_2 \theta_0') + (f_1' \theta_1 - f_1' \theta_1')\}$$

$$\frac{1}{\text{Pr}} \theta_n'' + \sum_{k=0}^n (1+k) f_k \theta_{n-k}' - \sum_{k=0}^n k \theta_k f_{n-k}' = 0$$

REFERENCES

- [1] Luciano M. De Socio, Laminar free convection around horizontal cylinders, *Int. J. Heat and Mass Transfer*, 26, No. 11, 1669-1677 (1983).
- [2], G. Cesini, M. Paroncini, G. Cortella, M. Manzan, Natural convection from horizontal cylinders in a rectangular cavity, *Int. J. Heat and Mass Transfer*, 42, 1801-1811 (1999).
- [3] M. A. Hossain, M. A. Alim, and D.A.S. Rees, The effect of radiation on Free convection from a porous vertical plate *J. Heat and Mass Transfer* 42, 181-191 (1999).
- [4] J. Ferziger, M. Peric, Computational methods for fluid dynamics, Springer Verlag, Berlin Heidelberg, 1996
- [5] S. V. Patankar, Numerical heat and mass transfer, McGraw-Hill Book Company
- [6] Bejan, Convective Heat Transfer, John Wiley & Sons, New York, 1984
- [7] A.A. Mohamad, Benchmark solution for unsteady state CFD problem, *Numerical Heat Transfer*, p.p.653-672, Vol.34, (1998)
- [8] M. A. Alim and A. K. M. Sadrul Islam , Separation points of mixed convection boundary layer flow along a vertical porous plate with exponentially decreasing free stream velocity, *Proc. International Conference on Fluid Mechanics and Heat Transfer*. ICFMHT-99, pp. 202-212, (1999).
- [9] T. Cebecci, P. Bradshaw, Physical and computational aspects of Convective heat transfer, Springer, New York, 1984.
- [10] H. J. Merk and J. A. Prins, Thermal convection laminar boundary layers I, II, *Appl. Scient. Res* A4, 11-24 (1954); 4, 195-206 (1954)

- [11] S. Sathe, B. Saminakia, A review of recent developments in some practical aspect of air-cooled electronic packages, *Transaction of ASME, Vol.120, Nov.(1998)*
- [12] M. A. Hossain, M. A. Alim, and D.A.S. Rees, Effects of thermal radiation on natural convection over cylinders of elliptic cross section, *Acta Mechanica Vol.129, 177-186 (1998).*
- [13] B. Farouk, S.I. Guceri, Natural convection from horizontal cylinder – laminar regime, *ASME J. Heat Transfer, Vol.103, (1981)*
- [14] T. H. Kuhen, R. J. Goldstein, An experimental study of natural convection heat transfer in concentric and eccentric horizontal cylindrical annuli, *J. Heat Transfer, vol. 100, (1978)*
- [15] S.H. Tasnim, S. Mahmud, Flow and thermal field behavior around an isothermal square cylinder in a large confined enclosure, *3rd Int. Conference on Fluid Mech. & Heat Transfer, ICFMHT-99, p.p.212-217, (1999)*
- [16] J.H. Merkin, Free convection boundary layers on cylinder of elliptic cross section, *Journal of Heat Transfer, Vol. 99, Aug. (1977)*
- [17] D. Naylor and J.D. Tarasuk, Natural convective heat transfer in a divided vertical channel: Part I—numerical study and Part II—experimental study. *Journal of Heat Transfer* 115 (1993), pp. 377-394.

